



Calhoun: The NPS Institutional Archive

Theses and Dissertations

Thesis Collection

2002-06

Verification of a 1-dimensional surf prediction model for steep beach conditions

Cutshaw, Charles Q.

Monterey, California. Naval Postgraduate School

<http://hdl.handle.net/10945/5940>



Calhoun is a project of the Dudley Knox Library at NPS, furthering the precepts and goals of open government and government transparency. All information contained herein has been approved for release by the NPS Public Affairs Officer.

Dudley Knox Library / Naval Postgraduate School
411 Dyer Road / 1 University Circle
Monterey, California USA 93943

<http://www.nps.edu/library>

NAVAL POSTGRADUATE SCHOOL

Monterey, California



THESIS

**VERIFICATION OF A 1-DIMENSIONAL SURF
PREDICTION MODEL FOR STEEP BEACH CONDITIONS**

by

Charles Q. Cutshaw, Jr.

June 2002

Thesis Advisor:
Second Reader:

Edward B. Thornton
Ad Reniers

Approved for public release; distribution is unlimited

THIS PAGE INTENTIONALLY LEFT BLANK

REPORT DOCUMENTATION PAGE			<i>Form Approved OMB No. 0704-0188</i>	
Public reporting burden for this collection of information is estimated to average 1 hour per response, including the time for reviewing instruction, searching existing data sources, gathering and maintaining the data needed, and completing and reviewing the collection of information. Send comments regarding this burden estimate or any other aspect of this collection of information, including suggestions for reducing this burden, to Washington headquarters Services, Directorate for Information Operations and Reports, 1215 Jefferson Davis Highway, Suite 1204, Arlington, VA 22202-4302, and to the Office of Management and Budget, Paperwork Reduction Project (0704-0188) Washington DC 20503.				
1. AGENCY USE ONLY (Leave blank)		2. REPORT DATE June 2002	3. REPORT TYPE AND DATES COVERED Master's Thesis	
4. TITLE AND SUBTITLE: Verification of a 1-Dimensional Surf Prediction Model for Steep Beach Conditions			5. FUNDING NUMBERS	
6. AUTHOR(S) LT Charles Q. Cutshaw Jr.				
7. PERFORMING ORGANIZATION NAME(S) AND ADDRESS(ES) Naval Postgraduate School Monterey, CA 93943-5000			8. PERFORMING ORGANIZATION REPORT NUMBER	
9. SPONSORING /MONITORING AGENCY NAME(S) AND ADDRESS(ES) N/A			10. SPONSORING/MONITORING AGENCY REPORT NUMBER	
11. SUPPLEMENTARY NOTES The views expressed in this thesis are those of the author and do not reflect the official policy or position of the Department of Defense or the U.S. Government.				
12a. DISTRIBUTION / AVAILABILITY STATEMENT Approved for public release; distribution is unlimited			12b. DISTRIBUTION CODE	
13. ABSTRACT (maximum 200 words) Wave breaking is the only source of energy dissipation in the Battjes and Janssen (1978) wave transformation model, which is parameterized by a breaking wave parameter, γ . The Battjes and Janssen (1978) wave transformation model was calibrated by Battjes and Stive (1985) and the calibration was refined by Morris et al. (2001) for waves over shallow sloping beaches. The objective of this study was to further refine the calibration to include steep beaches for a range of wave conditions by analyzing data from a nearshore experiment at Sand City, California. Waves were measured by a cross-shore array of nine pressure sensors. The pressure data were analyzed for H_{rms} and compared with calculated H_{rms} by the model. Results were largely inconclusive, which is attributed to wave reflection from the steep beach, something not accounted for in the model. Excluding data collected at low tides and allowing the model to account for reflection would likely reveal a more interesting outcome.				
14. SUBJECT TERMS Surf forecasting, surf model, waves, steep beach			15. NUMBER OF PAGES 41	
			16. PRICE CODE	
17. SECURITY CLASSIFICATION OF REPORT Unclassified	18. SECURITY CLASSIFICATION OF THIS PAGE Unclassified	19. SECURITY CLASSIFICATION OF ABSTRACT Unclassified	20. LIMITATION OF ABSTRACT UL	

THIS PAGE INTENTIONALLY LEFT BLANK

Approved for public release; distribution is unlimited

**VERIFICATION OF A 1-DIMENSIONAL SURF PREDICTION
MODEL FOR STEEP BEACH CONDITIONS**

Charles Q. Cutshaw, Jr.
Lieutenant, United States Navy
Undergraduate (B.A.), University of Washington, 1997

Submitted in partial fulfillment of the
requirements for the degree of

**MASTER OF SCIENCE IN METEOROLOGY AND PHYSICAL
OCEANOGRAPHY**

from the

**NAVAL POSTGRADUATE SCHOOL
June 2002**

Author: Charles Q. Cutshaw Jr.

Approved by: Edward B. Thornton
Thesis Advisor

Ad Reniers
Second Reader

Mary Batteen
Chairperson, Department of Oceanography

THIS PAGE INTENTIONALLY LEFT BLANK

ABSTRACT

Wave breaking is the only source of energy dissipation in the Battjes and Janssen (1978) wave transformation model, which is parameterized by a breaking wave parameter, γ . The Battjes and Janssen (1978) wave transformation model was calibrated by Battjes and Stive (1985) and the calibration was refined by Morris et al. (2001) for waves over shallow sloping beaches. The objective of this study was to further refine the calibration to include steep beaches for a range of wave conditions by analyzing data from a nearshore experiment at Sand City, California. Waves were measured by a cross-shore array of nine pressure sensors. The pressure data were analyzed for H_{rms} and compared with calculated H_{rms} by the model. Results were largely inconclusive, which is attributed to wave reflection from the steep beach, something not accounted for in the model. Excluding data collected at low tides and allowing the model to account for reflection would likely reveal a more interesting outcome.

THIS PAGE INTENTIONALLY LEFT BLANK

TABLE OF CONTENTS

I.	INTRODUCTION.....	1
II.	EXPERIMENT	3
III.	ANALYSIS	7
	A. WAVE TRANSFORMATION MODEL	7
	B. WAVE HEIGHT DATA.....	10
	C. COMPARISONS.....	11
IV.	RESULTS	13
V.	DISCUSSION	19
VI.	CONCLUSIONS	21
	LIST OF REFERENCES.....	23
	INITIAL DISTRIBUTION LIST	25

THIS PAGE INTENTIONALLY LEFT BLANK

LIST OF FIGURES

Figure 1.	Iribarren numbers for conditions used to calibrate BJ78.....	2
Figure 2.	Time series of H_{rms} (top) and period (bottom).....	3
Figure 3.	Bathymetry and instrument locations of RIPEX experiment. (Coordinates are centered at 36.61629093N, 121.85327237W.) From Reniers et al., (2002).....	4
Figure 4.	Modeled (solid line) versus measured (dashed line) H_{rms} with sensor locations (stars), setup, and depth (including tide) for big wave, high tide conditions.....	13
Figure 5.	Same as Figure 4 but for low tide.....	14
Figure 6.	Same as Figure 4 but for small waves.....	14
Figure 7.	Same as Figure 4 but for small wave, low tide conditions.....	15
Figure 8.	Increase in ADV #2 H_{rms} (solid line) over buoy H_{rms} (dashed line) on day 136 (May 16).....	15
Figure 9.	Modeled (solid line) versus measured (dashed line) H_{rms} with sensor locations (stars), setup, and depth (including tide) for small wave, low tide conditions showing under forecast shoaling.....	16
Figure 10.	Optimized gamma versus deep water wave steepness (s_0) overlain by BJ85 curve for optimal gamma (Equation 1).....	17
Figure 11.	Optimized gamma versus Iribarren Number (ξ) overlain by Morris' curve for optimal gamma (Equation 2).....	17

THIS PAGE INTENTIONALLY LEFT BLANK

ACKNOWLEDGMENTS

I would like to thank Professor Edward Thornton for his inexhaustible supply of patience. His support and encouragement were never in doubt. Even with many setbacks and delays, he kept me focused and motivated. I would also like to thank Ad Reniers and Mark Orzech for their assistance. They constantly made time to answer any question I had. Their input and advice made my thesis process a rewarding experience. There are others who have made my path to thesis completion smoother and I thank them all. Your availability on a moments notice is greatly appreciated. What I most appreciate from my NPS experience is that even with all I have learned, I realize how little I really know.

THIS PAGE INTENTIONALLY LEFT BLANK

EXECUTIVE SUMMARY

The nearshore wave transformation model by Battjes and Janssen, (1978) is part of the Delft-3D nearshore wave and current model being considered for rapid transition for use as the operational model. Wave breaking is the only source of energy dissipation in the model, which is parameterized by a breaking wave parameter, γ . The Battjes and Janssen (1978) model was calibrated by Battjes and Stive (1985) and the calibration was refined by Morris et al. (2001) for waves over shallow sloping beaches. The objective of this paper was to further refine the calibration to include steep beaches for a range of wave conditions by analyzing data from a nearshore experiment at Sand City, California. Waves were measured by a cross-shore array of nine pressure sensors. The pressure data were analyzed for H_{rms} and compared with calculated H_{rms} by the model. Results were largely inconclusive, which is attributed to wave reflection from the steep beach, something not accounted for in the model. Excluding data collected at low tides and allowing the model to account for reflection would likely reveal a more interesting outcome.

THIS PAGE INTENTIONALLY LEFT BLANK

I. INTRODUCTION

Prediction of sea surface elevation (SSE) due to breaking waves is an area of critical interest in a variety of fields including municipal planning and military operations. States, counties, and cities benefit from a reliable method of forecasting surf conditions in many areas such as safety of beach-goers and zoning restrictions. Military planners, especially Navy and Marine Corps personnel conducting amphibious operations and special operations, require accurate predictions of surf conditions.

The Battjes and Janssen (1978) waveheight model for surf prediction (hereafter referred to as BJ78) is compared with data acquired on a steep beach. The model has been successfully tested with data from beaches with gentle slopes. (Battjes and Stive, 1985) There are no known results of testing this model on steep beach conditions. The BJ78 model is the basis of wave prediction in the surf zone for the wave, current, and morphology model, DELFT3D, currently under consideration for transition to operational use for the U.S. Navy.

The model was first calibrated by Battjes and Stive (1985) for data having relatively steep waves and gentle beach slopes. The model has a breaking wave parameter (γ), which was shown to be dependent on deep-water wave slope (s_0) as given by

$$\gamma = 0.5 + 0.4 \tanh 33s_0 \quad (1)$$

where $s_0 = H_0/L_0$ in which H_0 is the offshore wave height, and L_0 is the offshore wave length.

Morris et al. (2001) expanded the calibration to include waves of low wave steepness (swell) and found an additional dependence on beach slope as given by

$$\gamma = 0.2 + 0.32 \tanh \xi \quad \text{for } s_0 < 0.002, \quad (2)$$

where ξ is the Iribarren number given by

$$\xi = \frac{\tan \beta}{s_0} \quad (3)$$

where $\tan \beta$ is the beach slope. The wave and beach geometry based on the Iribarren number for all of the comprehensive, large-scale nearshore field experiments is summarized in Figure 1. The data analyzed here is from the RIPEX experiment, which has not been previously analyzed. RIPEX data represent large Iribarren numbers for large beach slopes and swell conditions.

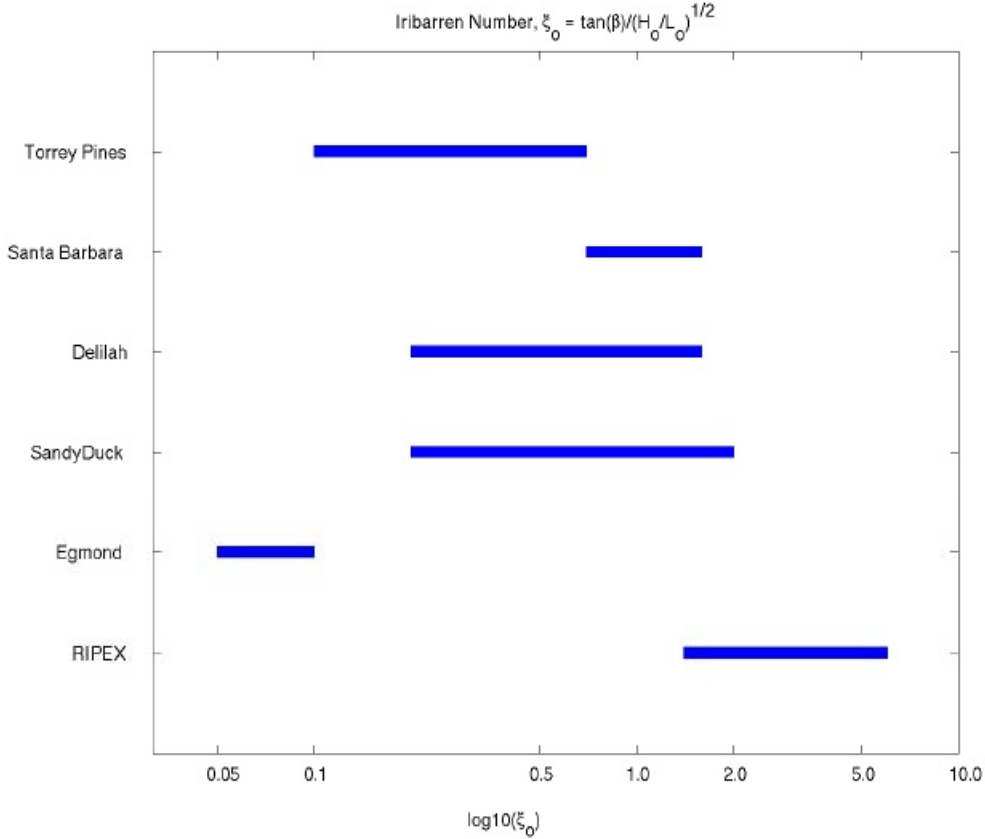


Figure 1. Iribarren numbers for conditions used to calibrate BJ78.

The objective of this paper is to calibrate the Battjes and Janssen (1978) model for steep beach conditions by finding the optimal γ values for model comparison with data. The next section of this paper discusses the experiment including location, time for which data were collected, sensors used to collect data, and conditions of the beach and surf. Following that is a description of the model and the methods used in this paper to analyze the data. The last two sections are results and conclusions.

II. EXPERIMENT

The Rip-Current Experiment (RIPEX) was conducted from 10 April to 22 May 2001 on a steep beach in Sand City, California. The beach steepness varied from 1:20 offshore graduating into a tidal plateau finally rising into a steep 1:5 beach face. Significant wave heights ranged from 0.5 to 2m with periods ranging from 5 to 17sec. (Figure 2) The waves approached at near normal incidence to the local shoreline due to severe refraction and a relatively narrow aperture caused by the sheltering headlands of Monterey Bay.

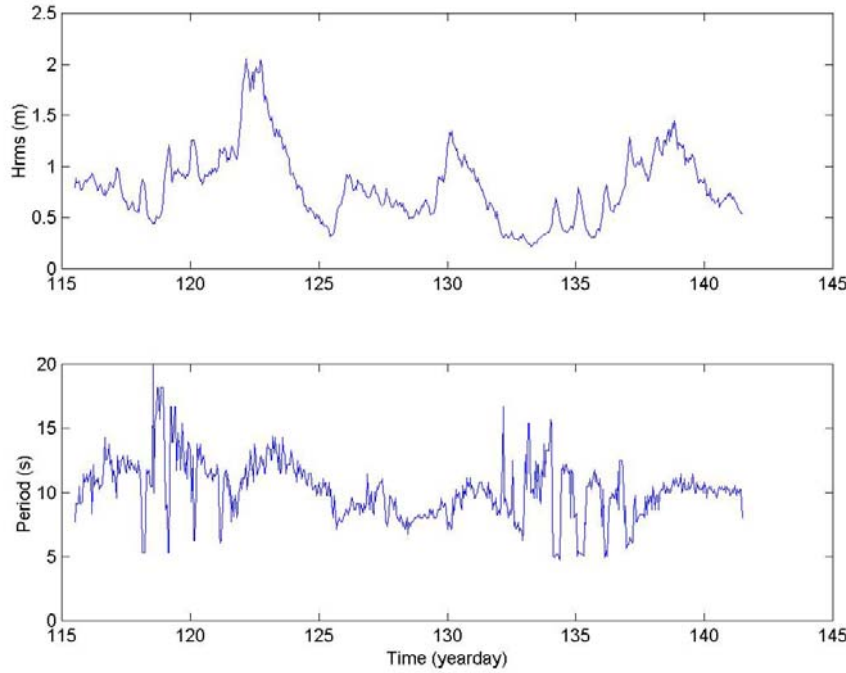


Figure 2. Time series of H_{rms} (top) and period (bottom)

Bathymetry data were collected from the base of the dunes out to a depth of 18m using three methods to obtain full coverage. On the beach, an all terrain vehicle (ATV) drove over the dunes with a Differential Global Positioning System (DGPS) receiver. Latitude, longitude, and elevation were recorded with horizontal and vertical accuracies with 6 cm rms error. A jet ski with an echo sounder and DGPS receiver measured bathymetry from offshore to a depth of about 1m. From the beach seaward to a water

depth of approximately 1m, a person with a DGPS backpack walked the nearshore. Bathymetry was measured on nine days during the experiment.

For data considered here, waves were measured with a cross-shore array of nine pressure sensors extending approximately 235m offshore to a depth of approximately 6m. In addition, an offshore wave buoy was located 642m offshore in 16m of water at 36.61955N, 121.85921W. (Figure 3)

Pressure sensors over the shoal were attached to poles and sunk vertically into the sand to depths of 0.5m to 1.0m. The pressure sensors were a silicon-on-sapphire submersible pressure transducer made by Hydracon Co., model number 2450-301. The pressure range was 0-25psia. The two furthest offshore pressure sensors were incorporated within SonTek 5MHz ADV Ocean Probes.

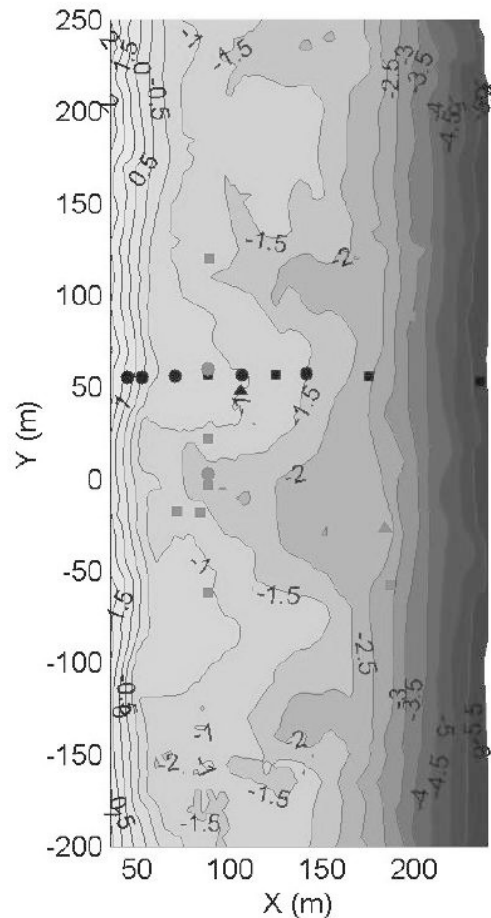


Figure 3. Bathymetry and instrument locations of RIPEX experiment. (Coordinates are centered at 36.61629093N, 121.85327237W.) From Reniers et al., (2002)

The wave buoy is a Directional Waverider Mark II, which measures wave height and direction. It is equipped with a heave-pitch-roll sensor Hippy-40. Directional data are accurate to within 1.5° with an error of 0.5° . Heave resolution is 1cm and accurate to 3% of the measured value. Frequency resolution is 0.005Hz from 0.025 to 0.1Hz and 0.01Hz from 0.1 to 0.59Hz. The high frequency cut-off is 0.6Hz.

THIS PAGE INTENTIONALLY LEFT BLANK

III. ANALYSIS

A. WAVE TRANSFORMATION MODEL

The transformation of waves from offshore to the beach is described using the energy flux balance model accounting for random wave breaking by Battjes and Janssen (1978). Assuming straight and parallel depth contours and stationary wave conditions, the energy flux balance is represented by

$$\frac{\partial E c_g \cos \theta}{\partial x} + D = 0 \quad (4)$$

where E is the mean wave energy, θ is the angle of the waves with respect to shore normal, x is the horizontal coordinate perpendicular to the shoreline, and D is the time-mean dissipated power per unit area, and c_g is the group velocity described by linear wave theory:

$$c_g = \left[\frac{2\pi f}{k} \left(\frac{1}{2} + \frac{kh}{\sinh 2kh} \right) \right]_{f=\bar{f}} \quad (5)$$

where h is depth, k is wavenumber, and \bar{f} is mean wave frequency of the assumedly narrow banded spectra. For simplicity it is further assumed that the only source of dissipation is wave breaking.

In deep water, random waves are well described as having a Rayleigh wave height distribution, which is a single parameter distribution in terms of the root mean square wave height (H_{rms}). Assuming linear wave theory, the mean energy density (E) for a Rayleigh wave height distribution is given by

$$E = 1/8 \rho g H_{rms}^2. \quad (6)$$

To describe wave breaking, it is assumed that if a random series of waves enters a given water depth (h), waves larger than a certain maximum height (H_m) will break and all waves shoreward of h will be equal in height or smaller than H_m . These waves are

described in terms of the clipped Rayleigh distribution of wave heights with a cutoff at H_m determined by h as given by

$$F(H) = 1 - \exp\left(-\frac{H^2}{2H_{rms}^2}\right) \quad \text{for } 0 \leq H \leq H_m$$

$$= 1 \quad \text{for } H_m \leq H.$$
(7)

The probability that at any given depth a wave height is from a broken or breaking wave is obtained from Equation (7), as

$$\frac{1 - Q_b}{\ln Q_b} = -\left(\frac{H_{rms}}{H_m}\right)^2$$
(8)

where Q_b gives the fraction of waves that are broken or breaking at any given depth. In deep water, $Q_b \rightarrow 0$. In shallow water, H_{rms}/H_m increases and, $Q_b \rightarrow 1$ implying that all waves have broken or are breaking, i.e. saturation. The breaking wave criterion (Miche, 1954) is assumed

$$H_m = 0.88k^{-1} \tanh(kh\gamma/0.88).$$
(9)

where γ is a coefficient that controls the fraction of breaking waves. As γ increases, H_m for a given depth increases, decreasing the amount of dissipation occurring at that location. This allows breaking to begin farther inshore. In shallow water, Equation (9) reduces to $H_m \cong \gamma h$.

Energy dissipation in a broken wave (D') is assumed to be similar to that of a linear bore. If the waves are periodic with mean frequency \bar{f} , then, for a single wave, the average power dissipated per unit area due to breaking is given as

$$D = \frac{D'}{L} = \frac{\bar{f}D'}{c} \cong \frac{\bar{f}D'}{\sqrt{gh}} \cong \frac{1}{4}\bar{f}\rho g \frac{H^3}{h}$$
(10)

where L is wavelength and c is phase speed.

To apply Equation (10) to random waves, it must be applied to broken waves only, where the broken waves are assumed to have a height equal to H_m and probability of occurrence of Q_b . Since most breaking occurs where $H_m \cong h$, H_m/h is dropped from the order of magnitude relationship and Equation (10) becomes

$$D = \frac{\alpha}{4} Q_b \bar{f} \rho g H_m^2 \quad (11)$$

where α is a constant of order one that controls the level of energy dissipation. By combining Equations (5) and (11), the rate of energy dissipated due to breaking waves can be expressed in terms of H_{rms} , depth (h), and constants.

The transformation of H_{rms} is obtained by integrating Equation (4) with known wave and depth profiles. In addition, the wave-induced time average water level change ($\bar{\eta}$) is calculated by solving the mean x-momentum flux balance as given by

$$\frac{dS_{xx}}{dx} + \rho g h \frac{d\bar{\eta}}{dx} = 0 \quad (12)$$

where the total depth is given as the sum of the still water depth, d , and set-up (-down)

$$h = d + \bar{\eta} \quad (13)$$

The cross-shore momentum flux for normally incident waves (also called radiation stress) is given by linear wave theory as

$$S_{xx} = \left(\frac{1}{2} + \frac{2kh}{\sinh 2kh} \right) E. \quad (14)$$

H_{rms} and peak period at ADV #2 for a given hour are used as initial conditions. Setup is assumed to be zero at ADV #2. The model calculates conditions every 2.5m starting one step shoreward of ADV #2. For each point's calculations, setup is initially assumed to be equal to the final setup of the previous point. The resulting calculated

setup is then added to depth and a change in setup is calculated. The model is iteratively run until the change in setup is less than 0.1% of depth, which includes bathymetry, tides and setup.

B. WAVE HEIGHT DATA

Wave heights are determined from pressure sensor data from April 25 to May 21, 2001. Data sampled originally sampled at 8Hz was decimated to 2Hz and separated into approximately one-hour segments and checked for non-periodic sampling times and gaps. The longest gap found in the data was 11 seconds. Linear interpolation was used to fill in the gaps.

The data were then checked for evidence of vertical movement of the pressure sensors. Vertical movement occurred when the sand about the mounting pipe liquefied owing to pipe vibration caused by pounding of the breaking waves. Vertical movement of the sensors was a concern especially for the sensors in shallow water. To check this, pressure sensor data were examined in two segments. The first was from April 25 to May 5. The second included data from May 5 to May 21. In each segment, a mean pressure was calculated over approximately every 50 seconds of data to filter out wave signature. The graphs of the resulting tidal variations were visually examined for two types of shifts: sudden vertical jumps corresponding to an equivalent of more than 10 percent of the water depth and gradual increasing or decreasing trends. No trends were found and only four sudden jumps of this magnitude were found.

To correct the data for the sudden jumps, mean seawater level was calculated prior to and after the sudden jumps and the difference added or subtracted to the post-jump data. This brought all data points from a given sensor to the same reference level. This type of shift occurred in the three pressure sensors closest to shore.

Sea surface elevation spectra (SSE) were calculated from pressure spectra using linear wave theory and applying one of two transfer functions. The transfer function for buried pressure sensors is given by Raubenheimer et al., (1998)

$$H(f) = e^{kz} \cosh(kh). \quad (15)$$

where z is the depth (positive downward) the sensor is buried in the sediment. For the ADV pressure sensors and at times when other sensors were not buried, the transfer function given by

$$H(f) = \frac{\cosh(kh)}{\cosh(k(h+z))} \quad (16)$$

was used to calculate SSE. If the depth of water over a pressure sensor was less than 5cm, no H_{rms} was calculated for that or any sensor closer to the beach.

The H_{rms} was calculated from the SSE spectra, $S_\eta(f)$, using

$$H_{rms} = 2\sqrt{2}\sigma \quad (17)$$

where $\sigma = \sqrt{\int_{0.05}^{0.3} S_\eta(f) df}$.

The deep-water waves H_{rms_0} were calculated by back-shoaling the wave height measured at the buoy, H_{rms_b} , to calculate s_0 ,

$$H_{rms_0} = H_{rms_b} \left(\frac{c_{g_b}}{c_{g_o}} \right)^{\frac{1}{2}} \quad (18)$$

where c_g is group velocity calculated using linear theory in Equation 5.

Measured bathymetry data were used to linearly interpolate bathymetry for days where no bathymetry data existed.

C. COMPARISONS

An optimal value for γ was determined for each one-hour run that gave the least error between the measured and modeled data. The error between the measured H_{rms} and each modeled H_{rms} were calculated for a range of γ between 0.25 and 0.9 in steps of 0.01, where the error was calculated as

$$e = \frac{1}{N} \sum_{i=1}^N \left[\frac{|H_{meas} - H_{mod}|}{H_{meas}} \right] \quad (19)$$

where N is the number of sensors in a run. If one of the sensors in either set of data had no value, that difference was ignored. Once the error was calculated for each γ run, an optimal γ was determined by the smallest error.

IV. RESULTS

Wave breaking was generally initiated approximately 180-200m offshore on the offshore slope depending on the tide elevation and the wave height. Once waves began breaking, they continued to break until they reached the beach. However, under high tide and small wave conditions, waves did not break until they reached the beach. (See Figures 4 through 7) Data from pressure sensors 1 through 3 and 6 showed many gaps due to exposure at low tides.

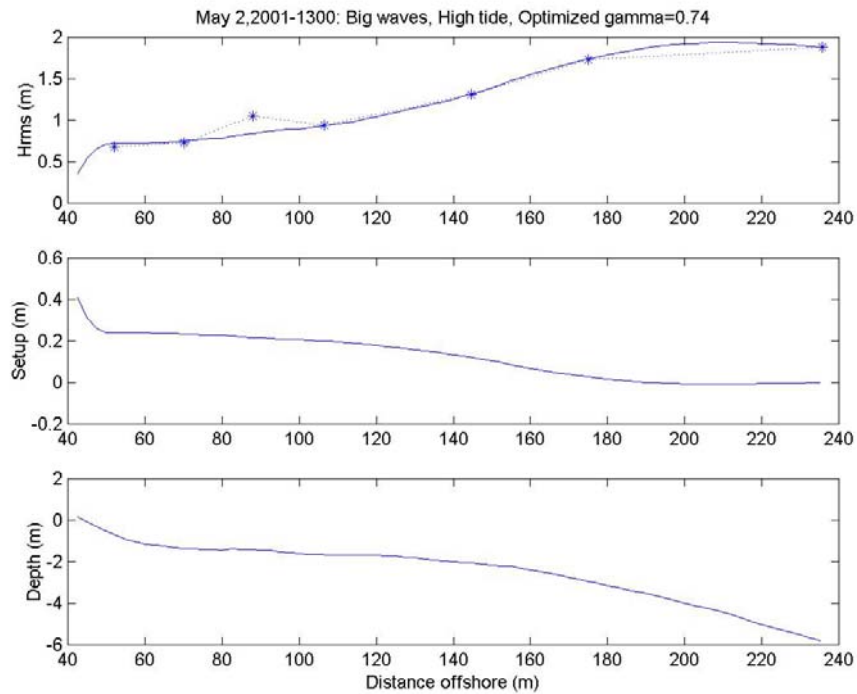


Figure 4. Modeled (solid line) versus measured (dashed line) H_{rms} with sensor locations (stars), setup, and depth (including tide) for big wave, high tide conditions

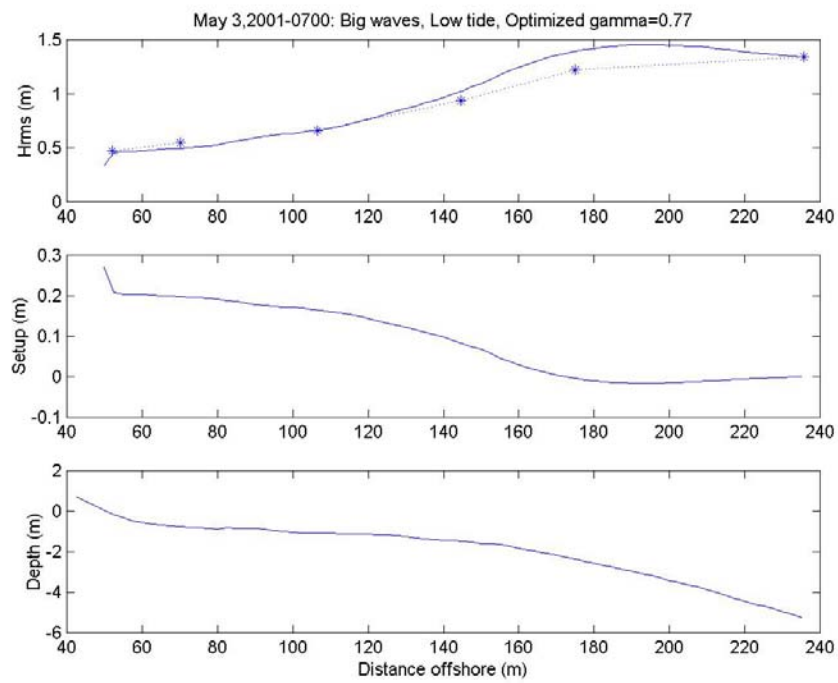


Figure 5. Same as Figure 4 but for low tide

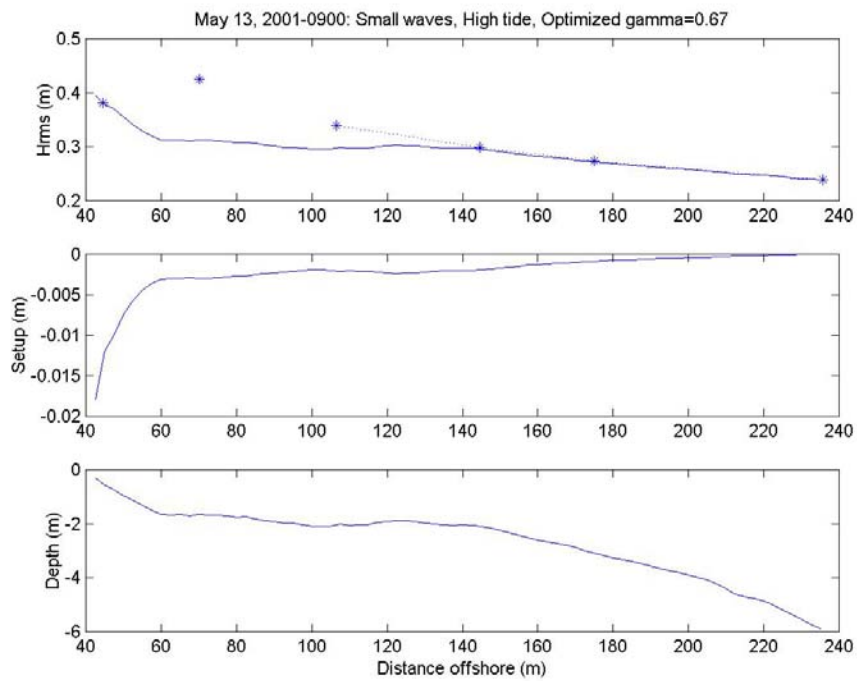


Figure 6. Same as Figure 4 but for small waves

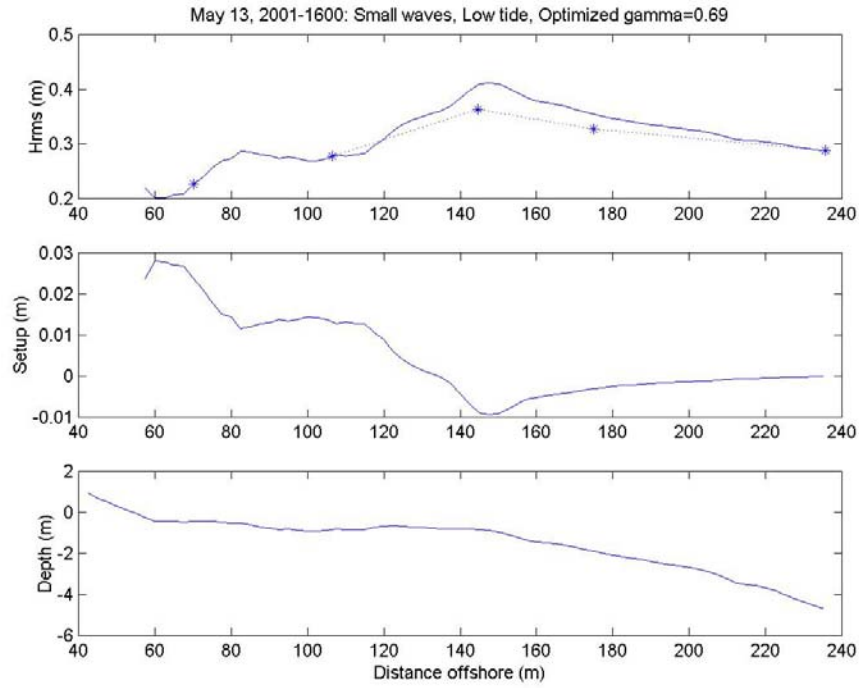


Figure 7. Same as Figure 4 but for small wave, low tide conditions

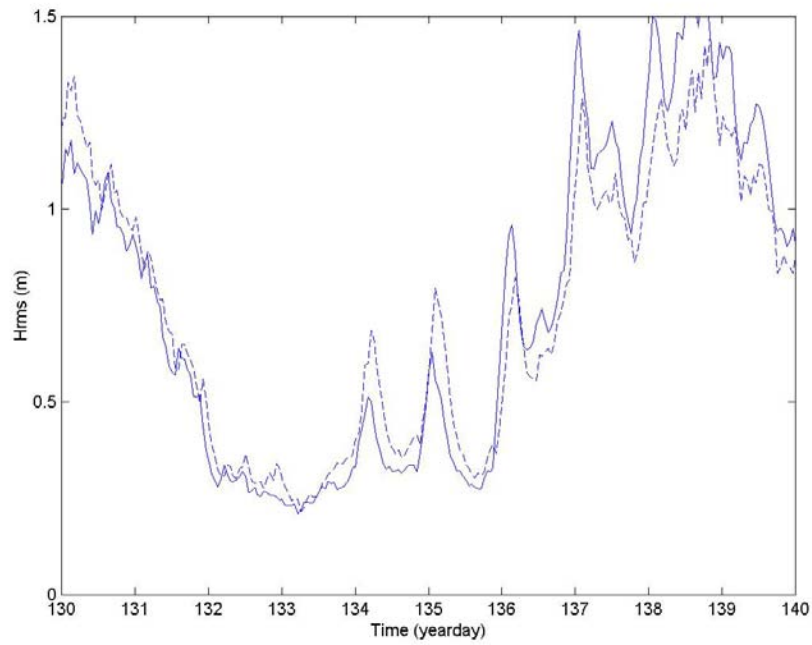


Figure 8. Increase in ADV #2 H_{rms} (solid line) over buoy H_{rms} (dashed line) on day 136 (May 16)

The modeled data agreed well with measured data, although the model sometimes did not model shoaling well. All errors associated with optimized gammas were less than 8 percent and the average error was 3 percent. At times shoaling was over-predicted (Figure 5) and at times under-predicted (Figure 9).

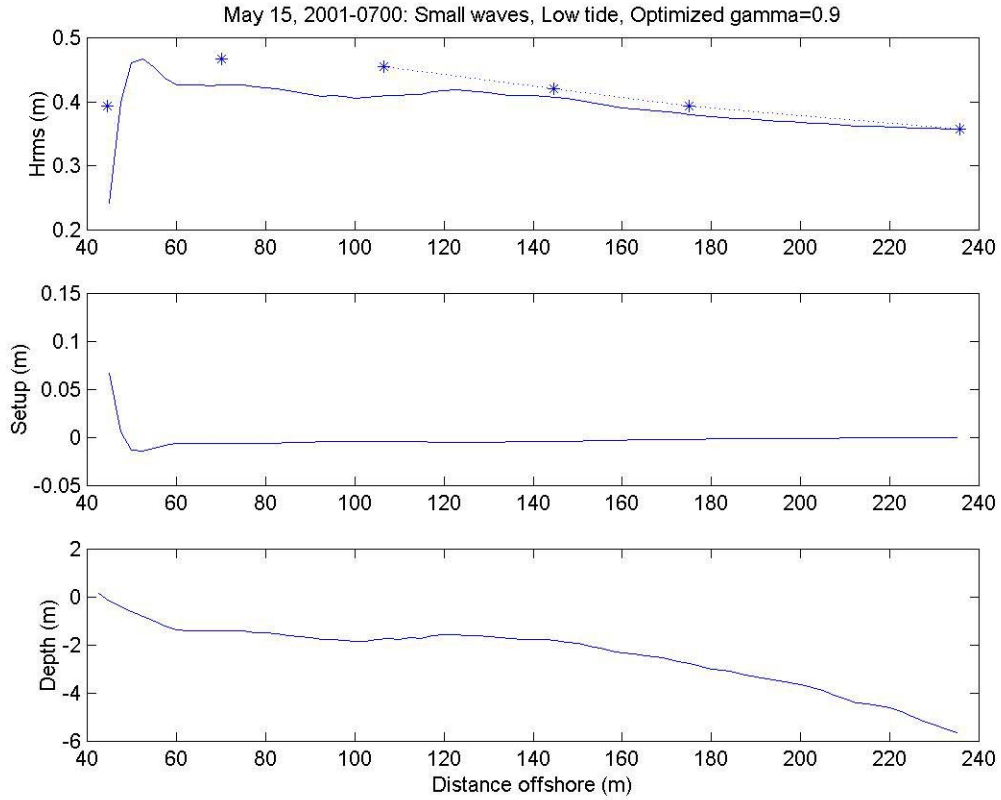


Figure 9. Modeled (solid line) versus measured (dashed line) H_{rms} with sensor locations (stars), setup, and depth (including tide) for small wave, low tide conditions showing under forecast shoaling

The optimized values of γ are plotted versus s_0 and Iribarren Number, (Figures 10 and 11). While the error was small, optimized gamma was scattered. The calibration curves as given by Equations (1) and (2) are plotted on each graph respectively for comparison purposes. Figures 10 and 11 show optimized gamma apparently reaching a maximum limit at 0.9. This is an artifact of limiting gamma to less than 0.9 which was considered greater than optimal gamma under any conditions.

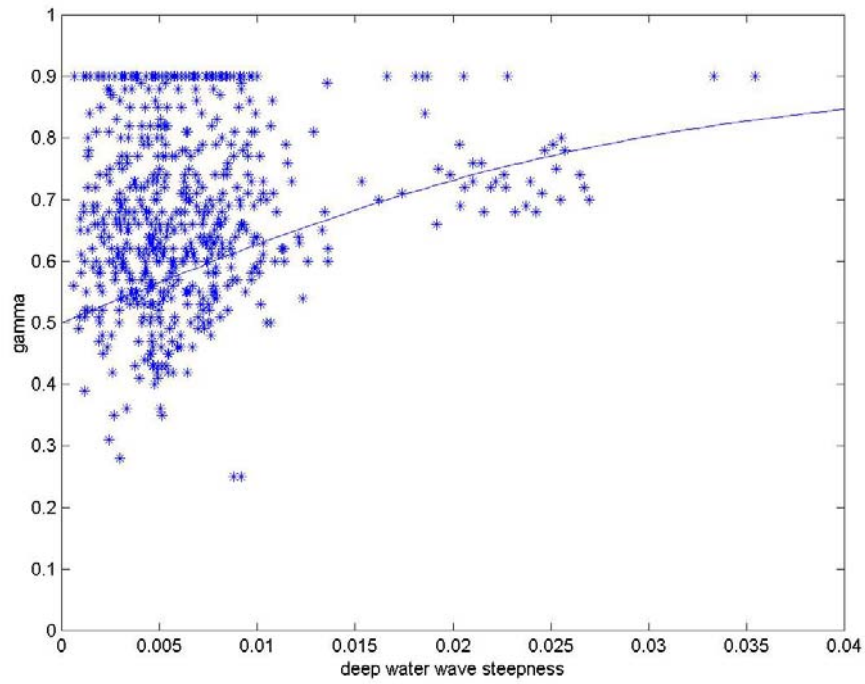


Figure 10. Optimized gamma versus deep water wave steepness (s_0) overlain by BJ85 curve for optimal gamma (Equation 1)

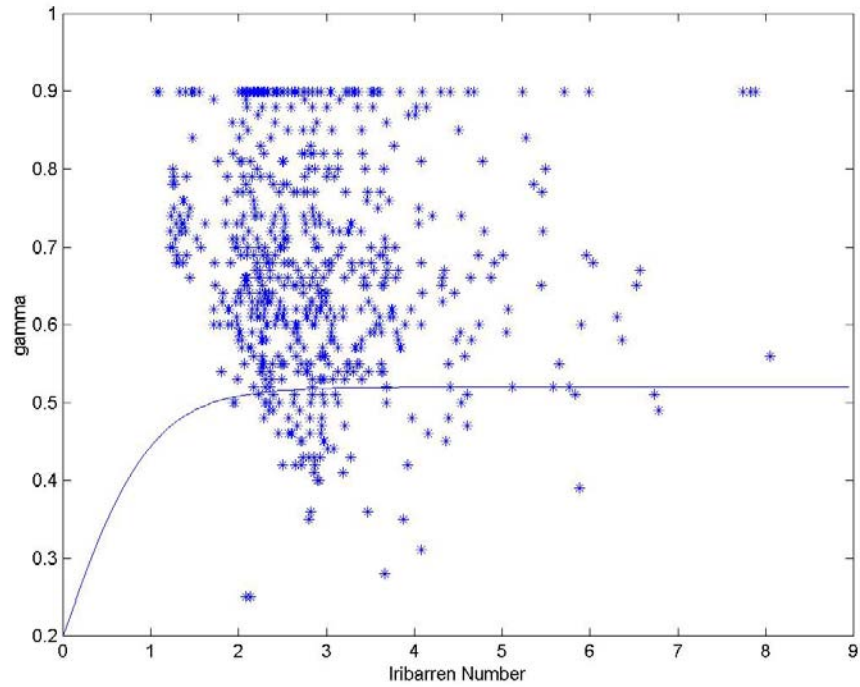


Figure 11. Optimized gamma versus Iribarren Number (ξ) overlain by Morris' curve for optimal gamma (Equation 2)

THIS PAGE INTENTIONALLY LEFT BLANK

V. DISCUSSION

The comparison of optimal γ as a function of both deep water wave steepness, s_0 , and Iribarren Number, ξ , show an unexpectedly large scatter. (Figures 10 and 11) The several points in Figure 10 with s_0 between 0.02 and 0.025 that are in good agreement with the BJ85 curve were compared with tides and wave height for some point of commonality but none was found.

No significant trends are seen in Figure 11. The significance of this is the same as described previously. However, since Iribarren Numbers were calculated with a beach slope of 1:5, these numbers may be incorrect at low tide when the tidal plateau is exposed. Time constraints prevented re-analyzing the measured data using only data taken at high tide. The models inability to handle shoaling consistently may be due to reflection from the beach. During some low tides, the tidal plateau was exposed. Reflection increases with beach slope. Reflection from the steep 1:5 beach was intermittent and occurred only on higher tides. Since the model does not account for reflection, this is a source of error. It was usually observed that the reflected and incident waves interacted to cause wave breaking when they collided with each other. Reflected waves would be expected to cause standing wave patterns that would modify how waves break. An example of small waves at high tide is shown in Figure 6 when strong reflection would be expected from the beach face, showing large differences between measurements and the model

ADV #2 gave H_{rms} larger than that of the seaward buoy after May 16. (Figure 8) ADV #2's increase in H_{rms} over that of the buoy was puzzling. A visual check of the pressure time series did not reveal a sudden jump as was observed in pressure sensors 1, 2, and 3. Its cause is unknown and another potential source of error.

THIS PAGE INTENTIONALLY LEFT BLANK

VI. CONCLUSIONS

The data analyzed for a barred, steep beach with low-slope incident swell waves did not compare well the calibration given by BJ85. Shoaling was erratically predicted in the model. Reflection is likely a source of error, which is not accounted for in the model. In order to achieve more conclusive and informative results from these data, they should be filtered so only those at high tide are considered. Additionally, reflection from the steep beach should be considered in the model.

THIS PAGE INTENTIONALLY LEFT BLANK

LIST OF REFERENCES

Battjes, J., and J. Janssen, (1978). Energy Loss and Set-up Due to Breaking of Random Waves. *Coastal Engineering*, 569-588.

Battjes, J., and M. Stive, (1985). Calibration and Verification of a Dissipation Model for Random Breaking Waves. *Journal of Geophysical Research*, 90 (C5) 9159-9160.

Miche, R. (1954). Mouvements Ondulatoires des Mers en Profondeur Constante ou Decroissante. *Ser. 3, Issue 363*. Wave Res. Lab., Univ. Calif. at Berkeley, Berkeley, CA.

Morris, B., E. Thornton, and A. Reniers, (2001). Calibration of a Random Wave Model to Long Period Swell., Doctoral dissertation, Naval Postgraduate School, Monterey, CA.

Raubenheimer, B., S. Elgar, and R. Guza, (1998). Estimating Wave Heights from Pressure Measured in Sand Bed. *Journal of Waterway, Port, Coastal, and Ocean Engineering*, 151-154.

Reniers, A., J. MacMahan, T. Stanton, and E. B. Thornton, (2002). Modeling of Infragravity Motions on a Complex Beach. In preparation.

THIS PAGE INTENTIONALLY LEFT BLANK

INITIAL DISTRIBUTION LIST

1. Defense Technical Information Center
Ft. Belvoir, Virginia
2. Dudley Knox Library
Naval Postgraduate School
Monterey, California
3. Edward B. Thornton
Naval Postgraduate School
Monterey, Ca
4. Ad Reniers
Naval Postgraduate School
Monterey, Ca